Figure 5 is a classified image of 2005 showing the distribution of the existing forest. The vegetation removed from the study area due to industrial expansion can be observed from Figure 6. Removal of the forest area was observed by comparing the classified image and the zones of expansion of industrial units extracted by the change detection from 2005 to 2011. Table 1 compares the loss of the existing forests in different categories. The total loss of forest in the area was found to be around 1265.36 ha from 2005 to 2011, with maximum expansion during 2005–2009 and within 5 km radius.

The zones of industrial expansion were verified on the ground (Figure 7) and the locations were found to match with the results extracted by change detection. It was found that large areas are being converted to non-forests due to industrial expansion. Figure 8 shows the ground photographs of some industrial units. The names of all the units are not been mentioned but the location of each unit as shown in Figure 7 constitutes the manufacturing unit, the mining area, etc. of several cement industries.

The present study has been carried out in a small area of radius 5 and 10 km to understand the ongoing changes in the immediate vicinity of the cement manufacturing units. It is observed that the changes are occurring in the immediate surroundings, particularly within the radius of 5 km, which is perhaps due to the expansion of the manufacturing units. Major changes are noticed from 2005 to 2009, while the expansion continued during 2009–2011. The expansion has been occurring in the forested region. The total loss of forest within a short span is found to be 1265.36 ha, which is supported and validated with the ground information. This study attempts to observe and extract the forest–non-forest conversion using automated software like DeltaCue and also indicates the ongoing deforestation taking place due to the establishment of such industrial units in the region. At the same time there is increase in mining activity where good forest areas existed in the past. On the ground, it is found that a conglomeration of the manufacturing unit exists in this region. Therefore, it is important to take the immediate necessary steps to control further expansion leading to change from forest to non-forest land-use categories.

1. Shreeranjan, *Perspectives on Development in Meghalaya*, SIRD Meghalaya, 2011.
2. KyntaNgap, H. B., *The Economy of Meghalaya – Tradition to Transition*, Spectrum Publications, 2001, p. 6.
3. IPCC special report on land use, land-use change and forestry, 2000, p. 4.
4. Sarma, S., *Meghalaya – The Land and Forest, a Remote Sensing Based Study*, Geophil Publishing House, 2003, p. 14.

ACKNOWLEDGEMENTS. I thank the Director, North Eastern Space Applications Centre, Umiam, for support, guidance and encouragement. I also thank INTERGRAPH Imagine software support team, Kolkata, for help.

Received 4 January 2014; revised accepted 8 March 2014

Hydrogeochemical assessment of groundwater in karst environments, Bringi watershed, Kashmir Himalayas, India

Nadeem A. Bhat[1,*], Gh. Jeelani[1] and M. Yaseen Bhat[2]

[1]Department of Earth Sciences, University of Kashmir, Srinagar 190 006, India
[2]Directorate of Geology and Mining, Srinagar 190 015, India

Hydrogeochemical assessment of precipitation, streams and springs of Bringi watershed, SE Kashmir has revealed that Ca and HCO_3 are the dominant ions, making up more than 50% of the total ions, which indicates carbonate lithology as the dominant source of ionic species. However, increased Na in some samples, particularly Kongamnag, indicates the impact of silicate weathering on water chemistry. The dominant order of cations and anions in the water samples is Ca > Mg > Na > K and HCO_3 > SO_4 > Cl respectively. In both streams and springs, electrical conductivity, total dissolved solids (TDS), Ca, HCO_3 are high during winter when the discharge is low and low during summer when the discharge is high. However, Kokernag and Achabalnag springs also show higher concentrations during July, resulting from piston effect. The springs show a significant variability of TDS, with highest value of 180 mg/l observed at Achabalnag followed by Kokernag (130 mg/l) and Kongamnag (90 mg/l). The high variability of TDS indicates rapid and strong reaction of Achabalnag to hydrological events followed by Kokernag and Kongamnag.

Keywords: Bringi watershed, hydrogeochemistry, Karst springs, Kashmir Himalayas.

NATURE has bestowed the Kashmir Valley with ample freshwater resources in the form of snow and glaciers, surface water and groundwater. Towards SE Kashmir, numerous freshwater springs are concentrated in Anantnag district[1] ('Anant' in Sanskrit language means countless and 'Nag' in the local language means springs), occurring along the foothills of Pir-Panjal range, controlled by limestone lithology[2]. Besides being of historical importance for decades, the spring water has been majorly used for domestic and agriculture purposes since prehistoric times.

As a result of chemical reaction between groundwater and carbonate minerals, the chemistry of groundwater changes from low mineralized to highly mineralized[3], particularly HCO_3, Ca and Mg (ref. 4) until a quasi-chemical equilibrium is reached[5]. The highly mineralized groundwater emerges at the surface in the form of a karst

*For correspondence. (e-mail: mnadeem83@gmail.com)

spring, provides information about the geology of the recharge areas[6], flow paths[3] and recharge environments[5]. Numerous studies have been carried out to examine the effect of source rocks over chemical composition of natural waters[7]. The studies have shown that chemical weathering of rocks in the drainage basin is largely controlled by carbonate dissolution[7,8]. The major ion chemistry thus acts as a powerful tool for determining source of solutes in groundwater[9], response of karst aquifers to hydrological events[10] and for describing evolution of water as a result of water–rock interaction, leading to the dissolution of carbonate minerals[11,12], silicate weathering[13] and ion-exchange processes[14].

In this communication, major ion chemistry of precipitation, surface and groundwater has been interpreted for better understanding of the mechanism of interactions and of the processes controlling the composition of surface water and groundwater, for making more informed environmental decision for protection of the valuable water resource of the region.

Bringi catchment, one of the main upland catchments of River Jhelum, lies towards the SE of Kashmir Valley in Western Himalayas between lat. 33°20′N and 33°45′N and long. 75°10′E and 75°30′E (Figure 1), covering an area of 595 sq. km. The elevation of this mountainous catchment ranges from 1650 m amsl at Achabal town to more than 4000 m amsl near Sinthan top. The Bringi watershed is drained by the Bringi stream which is fed by a number of tributaries, of which the important ones are east Bringi and west Bringi[15]. The streams are mostly fed by seasonal snow melt which generally lasts up to August and September. Bringi stream joins River Jhelum at Anantnag.

Three major springs occur in the Bringi watershed, namely Achabalnag, Kokernag and Kongamnag (Figure 1). At Achabalnag, water issues out from the base of Sosanwar hills[16] from two sites that are 150 m apart, with one major outlet carrying 75% of the total discharge. At Kokernag, water issues out from several places along a 50 m front at the base of a limestone hill and is channelled through a garden. At Kongamnag, water issues out from Karewas in the form of a pool, at the base of a limestone hill and is channelled through the surrounding villages.

The Bringi watershed has diverse rock types ranging in age from Palaeozoic sedimentary rocks to Recent alluvium[17–19], with Panjal Traps and Triassic Limestone as the dominant formations of hydrogeological importance (Figure 2). Upper Paleozoic rocks, lava, pyroclasts and arenites are only marginal to the study area, although they support most of the head-water drainage. Overlying these is a sequence of Triassic Limestone[18], though nowhere fully exposed, almost certainly more than 1000 m thick. The limestone is by no means pure and contains 15–90% dolomite with higher value being more spread[20]. In the vicinity of springs, the limestone is thinly bedded with shale partings present in most bedding planes, rarely more than 2 m apart. Horizons of shale and sandstone up to 5 m thick are also common throughout the succession. Karewas are the fluvio-lacustrine deposits that contain unconsolidated material like light grey sands, dark grey clays, coarse to fine-grained sand, gravel, marl, silt, varved clays and lignite[21]. The alluvial deposits comprise Recent sediments containing fine silt and mud, though active flood plains are mainly of coarse gravel and boulders[22]. Due to low hydraulic conductivity, alluvium and the Karewas block the water flowing through the Triassic Limestone and water appears in the form of a spring at the contact between soft rocks and Triassic Limestone.

Water samples from precipitation, snow melt, streams and springs were collected for the study of major ion chemistry on bimonthly basis from March 2008 to January 2009 across the Bringi watershed. The samples were collected following standard procedures[23–25]. For major ion analysis, 3 precipitation (rainwater) samples, 6 stream

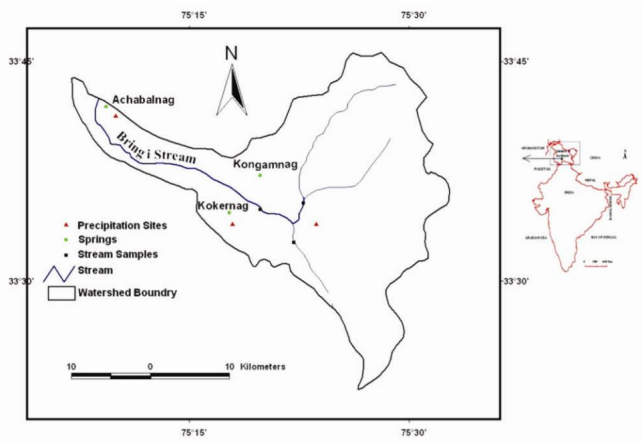

Figure 1. Location map of the study area along with sampling sites.

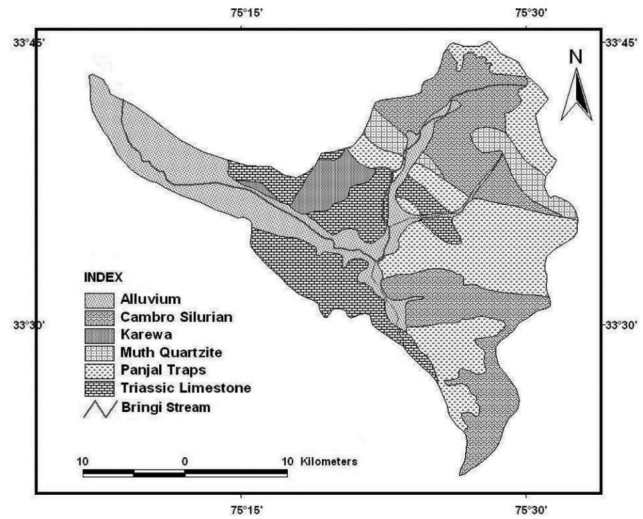

Figure 2. Geological map of the study area.

samples and 18 spring samples were collected in high-density polyethylene bottles (HDPE). To avoid the effect of floating debris, the stream and spring water samples were collected at depths greater than 30 cm below the water surface[24]. Prior to sample collection, the containers were washed with concentrated HNO_3 and completely rinsed with distilled water and then using the water that was to be sampled[23].

The master parameters such as water temperature, pH and electrical conductivity (EC) were determined *in situ*. Water temperature was measured by the standardized digital temperature meter (EI-421E), pH by the standardized digital pH meter (EI-432) and conductivity by standardized digital EC meter (EI-621). For major ion analysis, the samples were filtered through <0.45 μm nucleopore filter paper to separate the suspended sediments[26]. Major ion analysis was carried out in the Department of Earth Science and Department of Environment Science, University of Kashmir, Srinagar. Major ion analysis was carried out according to the standard methods[23]. Total dissolved solids (TDS) were determined by EC*0.64 (ref. 27). Ca^{2+} and Mg^{2+} were determined by EDTA titration using murexide as indicator, whereas Cl^- estimation was done by titrating the samples against $AgNO_3$ (0.02 N) using potassium chromate (5%) as an indicator. HCO_3^- was determined by titration of the water sample against HCl (0.01 N) in which methyl orange was used as an indicator. Na^+ and K^+ concentration in the samples was determined using flame emission photometer (Systronics-130). SO_4^{2-}, F^-, SiO_2^- and NO_3^- were determined by UV-VIS spectrophotometer (EI-1371).

The results of physico-chemical parameters of water samples are presented in Table 1. The precipitation samples are alkaline in nature with pH ranging from 8.6 to 8.9 at an average of 8.75. EC ranges from 64 to 78 μS/cm with a mean of 70 μS/cm. Chemical analysis of the precipitation water demonstrated a narrow range of salinity (TDS; 41–50 mg/l) at an average of 46 mg/l. Precipitation samples showed cation order as Ca (66%) > Mg (21%) > Na (12%) > K (1%) and anion order as HCO_3 (83%) > SO_4 (10%) > Cl (7%). The concentration of different cations and anions in precipitation can be attributed to the dissolution of different gases and dust content by atmospheric precipitation[26]. However, the high content of calcium and bicarbonates may also be due to stone crushers and cement industries located in the study area. The industries use limestone for cement production, which results in high emission of limestone dust into the atmosphere.

The temperature of the streams corresponds to the ambient temperature, ranging from 9.6°C to 17.4°C, with an average of 12.48°C. Stream water samples are moderately alkaline to alkaline in nature with pH ranging from 7.8 to 9.8 with an average of 8.2. EC ranges from 140 to 235 μS/cm, with an average of 175 μS/cm. TDS in the stream water samples vary from 89 to 193 mg/l with a mean of 122 mg/l. About 50% of the samples show cation order as Ca (61%) > Mg (26%) > Na (12%) > K (1%) and anion order as HCO_3 (89%) > Cl (7%) > SO_4 (4%). The other 50% of samples show cation order as Ca (62%) > Na (21%) > Mg (13%) > K (4%) and anion order as HCO_3 (88%) > SO_4 (8%) > Cl (4%).

The springs of the study area are fresh, colourless and odourless. Temperature of the springs ranges from 8.2°C to 14.4°C with an average of 12.2°C. Achabalnag and Kokernag show greater annual variability of temperature (~5.4°C and ~3.8°C) compared to Kongamnag with a variability of 1.7°C. The difference in variability in water temperatures may be attributed to shorter route of water at Achabalnag and Kokernag and longer route at Kongamnag. All the springs of the study area are neutral to moderately alkaline with pH ranging from 7.0 to 8.2, with an average of 7.6. EC of the springs ranges from 142 to 520 μS/cm, with an average value of 314 μS/cm. Highest EC is observed in Kongamnag during March and lowest in Achabalnag during May. TDS in the spring water samples of Bringi catchment ranges from 90 to 339.2 mg/l, with a mean of 206 mg/l. Highest concentration of TDS is observed in Kongamnag during March and lowest concentration is observed in Achabalnag during May. However, like EC, Achabalnag and Kokernag also show increased TDS during July. About 89% of water samples show order of cations as Ca (54%) > Mg (30%) > Na (15%) > K (1%) and 11% of samples show an order of Ca (53%) > Na (26%) > Mg (20%) > K (1%). Ca^{2+} is dominant among the cations. About 78% of samples show anion order as HCO_3 (86%) > SO_4 (10%) > Cl (4%) and 22% of samples show an order of HCO_3 (92%) > Cl (5%) > SO_4 (3%).

The major ion chemistry of groundwater is a powerful tool for determining solute sources and for describing water evolution as a result of water–rock interaction leading to the dissolution of carbonate minerals, silicate weathering and ion-exchange processes[14,27–29]. In order to understand the source of the solutes in a broader perspective, the hydrochemical data are plotted in the Gibbs diagram[30] (Figure 3). All the stream and spring water samples fall in the rock dominance area of the plot, which suggests that chemical weathering of the rock-forming minerals is the main process contributing ions to surface and groundwater. According to Piper trilinear diagram[31] (Figure 4), the order of four hydrochemical water types identified is Ca–Mg–HCO_3 > Ca–HCO_3 > Ca–Mg–Na–HCO_3 > Ca–Na–HCO_3. The water types have result from the congruent dissolution of carbonate-hosted lithology. The evolution of surface water is observed to be simple with all streams changed into Ca–Mg–HCO_3 water type due to easy dissolution of carbonate minerals and less time for water–rock interaction. However, as the water infiltrates downwards, more and more chemical constituents are added and groundwater evolves and modifies to different water types depending upon the flow path and

Table 1. Analytical data, calculated values, and statistical parameters of precipitation, streams and springs of the study area

Sample type	Sample date and no.	Statistics	Temperature (°C)	pH	EC (μS/cm)	(mg/l) TDS	SiO_2	F^-	NO_3^-	(mmol/l) Ca^{2+}	Mg^{2+}	Na^+	K^+	HCO_3^-	SO_4^{2-}	Cl^-	Ca/Mg
Precipitation	March–July 2008, $N = 3$	Minimum	NA	NA	64.0	41.0	NA	NA	1.38	0.10	0.04	0.01	0.0002	0.26	0.02	0.01	2.6
		Maximum	NA	NA	78.0	50.0	NA	NA	1.73	0.14	0.05	0.03	0.0005	0.30	0.05	0.04	3.5
		Mean	NA	NA	69.7	44.5	NA	NA	1.55	0.12	0.04	0.02	0.0003	0.28	0.03	0.02	3.06
		Standard deviation	NA	NA	7.4	4.2	NA	NA	0.17	0.02	0.00	0.01	0.0001	0.02	0.01	0.01	0.44
Streams	March 2008 to January 2009 $N = 6$	Minimum	9	7.8	140	89	0.2	0.8	0.35	0.29	0.04	0.09	0.0002	0.69	0.03	0.01	2.01
		Maximum	17.4	9.8	235	150.4	1.7	1.4	4.2	0.81	0.40	0.10	0.03	2.13	0.16	0.16	8.7
		Mean	12.4	8.3	174.7	110.7	1.2	1.0	1.61	0.42	0.15	0.10	0.02	1.12	0.07	0.06	3.96
		Standard deviation	3.3	0.8	38.2	25.4	0.5	0.3	1.53	0.19	0.13	0.01	0.01	0.53	0.05	0.05	2.54
Springs	March 2008, $N = 3$	Minimum	10.9	7.1	200	128	1.04	0.83	0.65	0.51	0.18	0.09	0.0002	1.15	0.08	0.09	1.2
		Maximum	13.1	7.6	530	339.2	1.6	0.9	3.18	0.96	0.80	0.57	0.0005	3.61	0.19	0.19	3.32
		Mean	11.7	7.3	314.0	201.0	1.3	0.85	2.0	0.69	0.41	0.30	0.0004	1.97	0.14	0.15	2.22
		Standard deviation	1.2	0.3	187.2	119.8	0.3	0.04	1.27	0.24	0.34	0.25	0.0001	1.42	0.06	0.05	1.06
	May 2008, $N = 3$	Minimum	11.2	7.4	142	90.88	0.5	0.82	1.25	0.24	0.16	0.10	0.001	0.74	0.12	0.07	1.33
		Maximum	13	8	442	282.8	0.7	0.86	4.2	0.92	0.48	0.52	0.003	2.79	0.13	0.17	2.00
		Mean	12.2	7.7	243.3	155.7	0.6	0.84	2.9	0.49	0.27	0.26	0.002	1.42	0.13	0.11	1.74
		Standard deviation	0.9	0.3	172.1	110.1	0.1	0.02	1.5	0.37	0.18	0.23	0.005	1.18	0.01	0.05	0.36
	July 2008, $N = 3$	Minimum	10.4	7.2	236.0	151.0	0.5	0.82	1.2	0.55	0.16	0.09	0.001	1.56	0.04	0.01	0.98
		Maximum	14.3	7.8	454.0	290.6	0.75	1.25	4.55	0.92	0.76	0.58	0.003	3.03	0.17	0.10	4.19
		Mean	12.8	7.4	338.7	216.7	0.6	1.09	3.06	0.74	0.38	0.27	0.002	2.24	0.11	0.04	2.88
		Standard deviation	2.1	0.3	109.6	70.1	0.15	0.23	1.7	0.18	0.33	0.27	0.001	0.74	0.07	0.05	1.68
	September 2008, $N = 3$	Minimum	12.0	7.0	222.6	142.5	0.7	0.62	0.85	0.63	0.24	0.11	0.003	1.47	0.03	0.02	1.15
		Maximum	14.4	7.7	448.0	286.7	1.9	0.72	5.75	0.80	0.70	0.65	0.005	3.20	0.37	0.23	2.64
		Mean	13.4	7.3	319.7	204.6	1.2	0.65	3.4	0.71	0.41	0.32	0.004	2.13	0.18	0.10	2.07
		Standard deviation	1.2	0.4	115.9	74.2	0.6	0.05	2.45	0.09	0.25	0.29	0.0009	0.93	0.17	0.12	0.81
	November 2008, $N = 3$	Minimum	11.9	7.3	212.2	135.8	0.6	0.74	0.72	0.34	0.36	0.13	0.002	1.23	0.10	0.04	0.94
		Maximum	14.3	8.1	454.8	291.1	1.7	0.96	5.0	0.86	0.72	0.24	0.005	3.44	0.27	0.22	1.2
		Mean	13.3	7.6	305.7	195.7	1.0	0.85	3.34	0.57	0.50	0.19	0.0025	2.02	0.19	0.11	1.11
		Standard deviation	1.2	0.4	130.5	83.5	0.6	0.11	2.29	0.27	0.19	0.06	0.001	1.23	0.09	0.10	0.14
	January 2009, $N = 3$	Minimum	8.2	7.6	280.2	179.3	0.17	0.86	0.68	0.81	0.34	0.11	0.004	1.97	0.03	0.04	1.38
		Maximum	12.0	8.2	520.2	332.9	1.7	0.96	4.2	1.16	0.84	0.23	0.006	3.93	0.09	0.18	2.4
		Mean	9.7	7.9	367.5	235.2	0.7	0.9	2.89	0.93	0.53	0.17	0.005	2.68	0.06	0.09	1.93
		Standard deviation	2.0	0.3	132.7	84.9	0.9	0.05	1.92	0.20	0.27	0.06	0.001	1.09	0.03	0.08	0.52

host lithology[5]. The water samples are also plotted in Langelier–Ludwig diagram[32] (Figure 5). Surface water and spring water are characterized by one main trend, i.e. carbonate dissolution. The plot shows that the spring and stream water samples are dominated by the carbonate dissolution with Ca–Mg–HCO_3 as the principal water type observed in most of the karst springs and streams of the study area.

To understand the major lithological source for the solutes in water samples, various scatter plots were drawn. In (Ca + Mg) versus HCO_3 (Figure 6 *a*), the data points of the stream water samples fall close to the equiline, indicating the dissolution of carbonate lithology as the dominant process of solute acquisition. However, the deviation of some spring water samples from the equiline indicates some other source for HCO_3. In the scatter plot (Ca + Mg) versus (Na + K) (Figure 6 *b*), the data points fall well below the equiline suggesting carbonate lithology as dominant source of major ions. The excess concentration of (Na + K) over (Ca + Mg) in some spring water samples (Kongamnag) indicates the impact of silicate lithology. The contribution from silicate rocks cannot also be ruled out because of their widespread distribution in the study area. In the plot (Na + K) versus Cl^- (Figure 6 *c*), most of samples fall above the equiline indicating some extra source of Na (K being very less and almost having homogeneous values). Figure 6 *b* and *c* favours the role of silicate weathering in the contribution of some major ions, particularly Na.

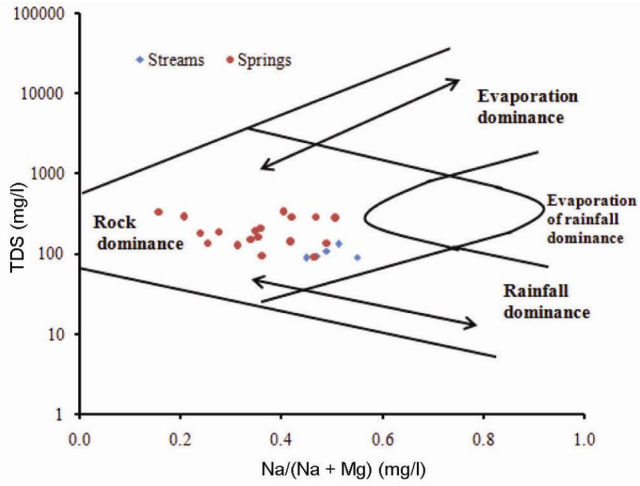

Figure 3. Gibbs diagram (after Gibbs[30]).

Ca/Mg molar ratios in the surface and spring waters of the study area averaged at 4.6 (range = 2.7–10) and at 1.99 (range = 1.1–2.2) respectively. In the surface water samples, the molar ratios are high in November (5.2) and low in March (2.7), whereas in groundwater samples the molar ratios are high in July (2.9) and low in May (1.7). The high variability of the Ca/Mg molar ratio in surface waters indicates various sources of Ca and Mg, including carbonates and silicates during different seasons. As all the water samples are undersaturated with calcite and dolomite[7], the variation in Ca/Mg molar ratio seems to be dependent on the lithogenic source. Low molar ratio is attributed to the weathering of silicates and/or dolomite, and high molar ratios can result from calcite weathering.

The plot Ca/Mg versus Mg (Figure 7 *a*) shows decrease in molar ratio with increase in Mg concentration, indicating dolomite weathering as the source of Ca and Mg. In the Ca/(Ca + Mg) versus $SO_4/(SO_4 + HCO_3)$ plot (Figure 7 *b*), all the surface water and most of the spring water samples are characterized by high Ca/(Ca + Mg) molar ratio indicating that the waters react mainly with calcite. However, the spring waters with intermediate values

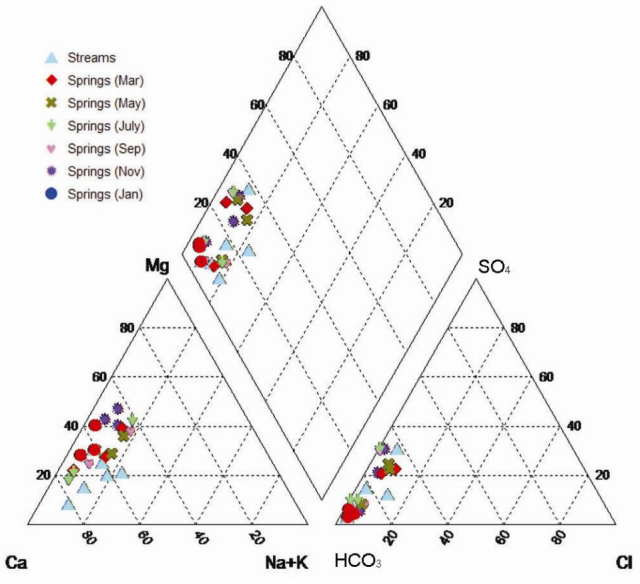

Figure 4. Piper trilinear diagram (after Piper[31]).

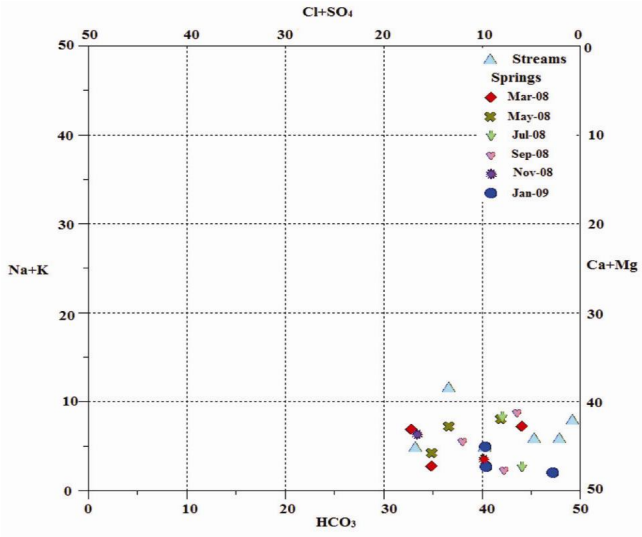

Figure 5. Langlier–Ludwig square diagram (after Langelier and Ludwig[32]).

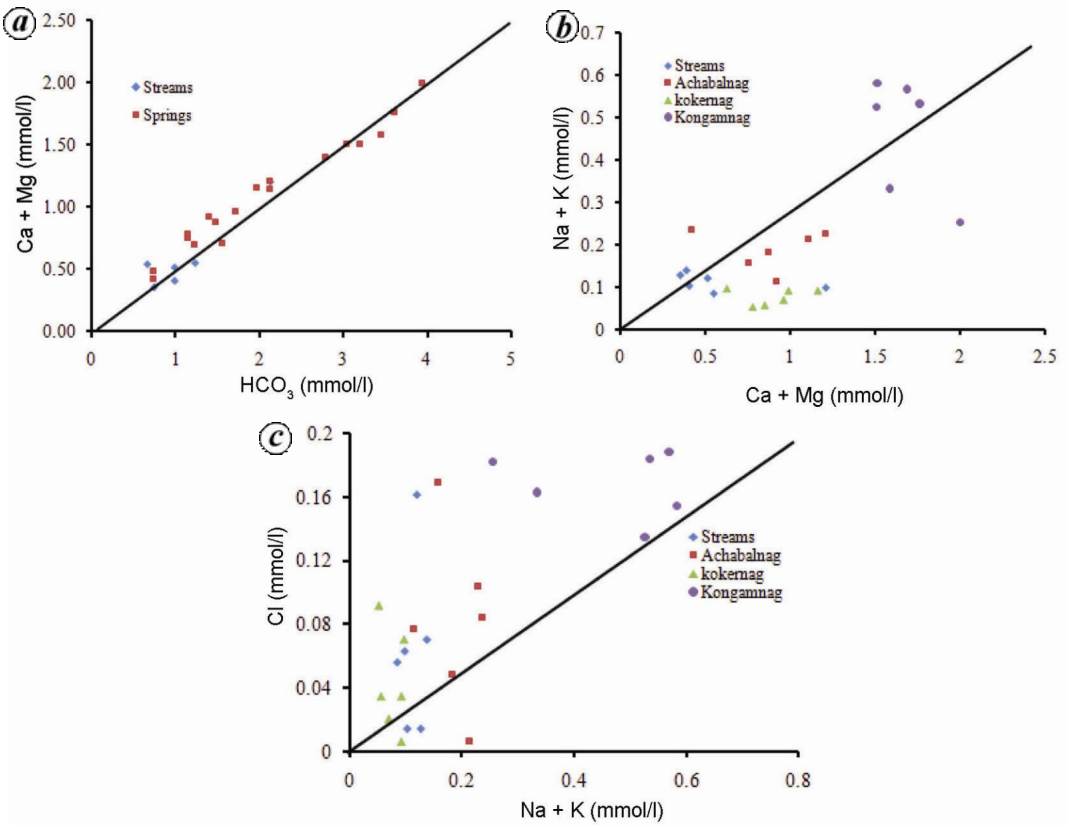

Figure 6. Scatter plots showing possible source of ionic species in springs. ***a***, (Ca + Mg) versus HCO_3. ***b***, (Ca + Mg) versus Na + K. ***c***, (Na + K) versus Cl.

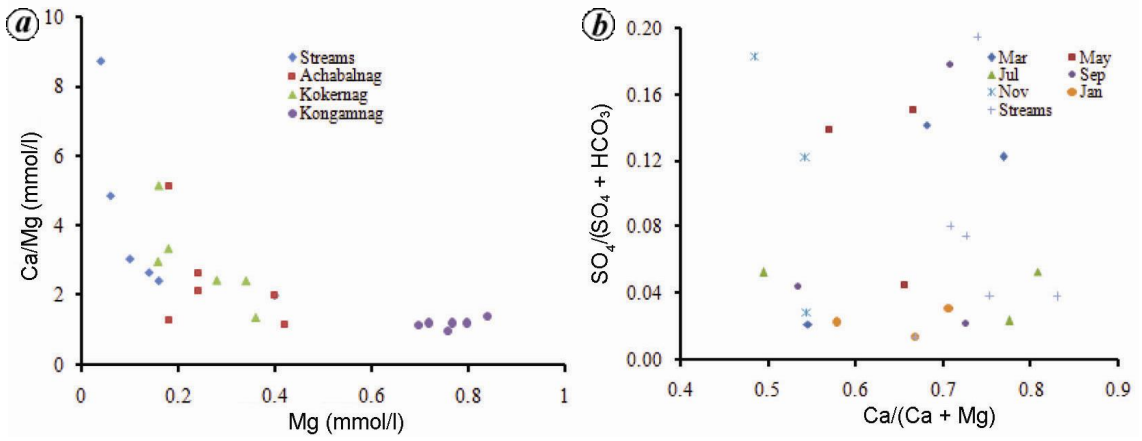

Figure 7. Scatter plots showing possible source of ionic species in springs. ***a***, Ca/Mg versus Mg. ***b***, Ca/(Ca + Mg) versus $SO_4/(SO_4 + HCO_3)$.

indicate the interaction with dolomite as well, particularly in May when recharge due to the melting of snow is at its peak. The Ca/(Ca + Mg) molar ratios of 0.5 and 1 correspond to the dissolution of stoichiometric dolomite and pure calcite respectively[33]. The relative increase in Mg with the increase in SO_4 in stream water samples, suggests the simultaneous process of dedolomitization and the gypsum and/or anhydrite dissolution.

Results of the physico-chemical analysis suggest that the karst springs and the Bringi stream have similar chemical composition. However, there are subtle differences in major ion chemistry between the springs. Achabalnag and Kokernag located at lower altitudes have less ionic concentration compared to the high-altitude spring (Kongamnag). At Kongamnag time of contact of water with the bedrock is more compared to Achabalnag and

Kokernag, which has resulted in high concentration of ions at Kongamnag. Water temperature both in streams and springs shows a distinguishable summer maximum and winter minimum. Similarly, the discharge of streams and springs begins to rise in spring attaining a maximum in summer, indicating enhanced recharge associated mainly with the melting of snow and a low during winter and spring reflects the low percolation rate during cold period (Figure 8). Frost action and to a large extent accumulation of precipitation on the surface in the form of snow mainly results in lower recharge rates during winters.

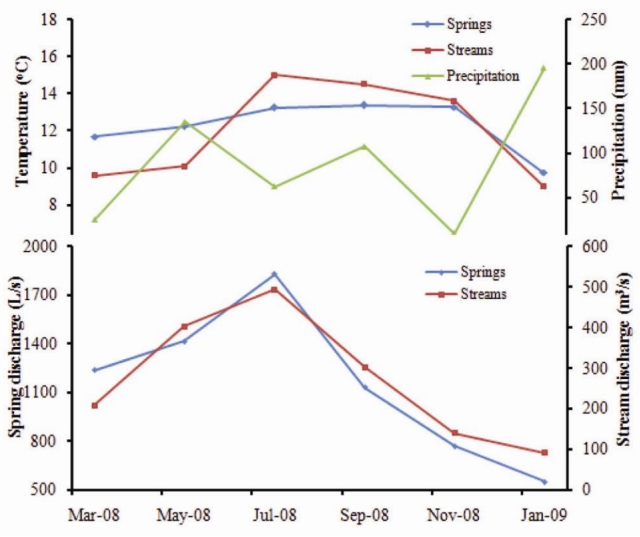

Figure 8. Variation of stream and spring temperature, discharge and precipitation.

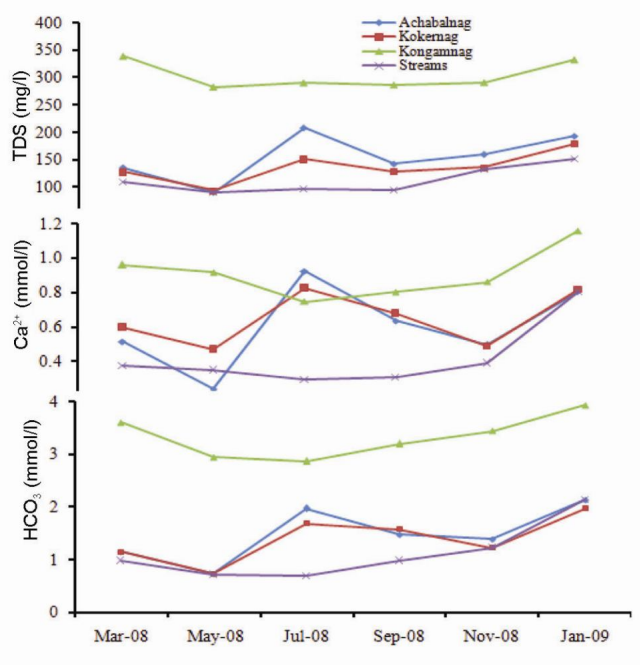

Figure 9. Positive correlation of TDS, Ca and HCO_3 between karst springs and Bringi stream.

In both streams and springs, Ca^{2+} and HCO_3^- are the dominant ions making up more than 50% of the ionic concentration. The chemographs of TDS, Ca^{2+} and HCO_3^- plotted between streams and springs show that the concentration of ions is high during March and January and low during the rest of the months (Figure 9). During March and January, because of frost action and less groundwater recharge, there is more residence time of groundwater which has resulted in prolonged rock–water interaction and thus more ions are acquired. On the other hand, during summer there is significant groundwater recharge and less residence time of groundwater which has resulted in low rock–water interaction, which lowers the dissolved ions in springs. However, in Achabalnag and Kokernag, the ions also show high concentration during July which may have resulted from the piston effect.

The plot of TDS versus spring discharge (Figure 10) shows that in July both discharge and TDS increase simultaneously. This observation indicates the arrival of highly mineralized water from deeper zone of the aquifer due to increased hydraulic pressure in the aquifer. Such a behaviour is not observed in Kongamnag, which indicates the slow movement and longer residence time of water compared to other springs. The chemographs plotted during different months for streams and springs show a positive correlation, which indicates that springs are fed by Bringi stream at different elevations. Further, the springs also show variability in their TDS with a significant variability at Achabalnag (~180 mg/l), followed by Kokernag (~130 mg/l) and Kongamnag (~90 mg/l), which indicates that Achabalnag reacts more rapidly and strongly to hydrological events followed by Kokernag and Kongamnag.

Chemical analysis of the precipitation water as well as stream and spring water samples revealed that Ca^{2+} was the dominant cation followed by Mg^{2+}, Na^+ and K^+. Among the anions, HCO_3^- was the most dominant followed by SO_4^{2-}, Cl^- and NO_3^-. The order of four hydrochemical water types identified was Ca–Mg–HCO_3 > Ca–HCO_3 > Ca–Mg–Na–HCO_3 > Ca–Na–HCO_3 it suggests congruent dissolution of carbonate-hosted lithology. The

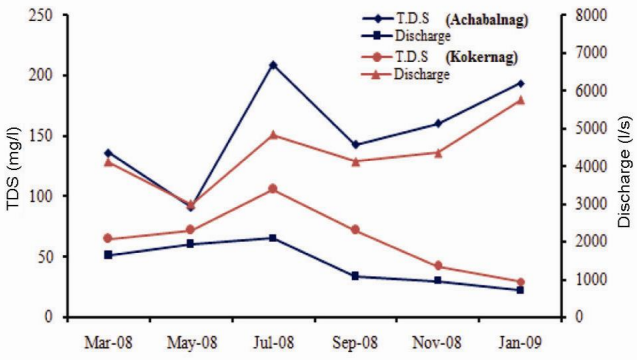

Figure 10. Relationship of TDS at Kokernag and Achabalnag with spring discharge depicting piston effect.

evolution of surface water is observed to be simple with all streams changed into Ca–Mg–HCO_3 water type due to easy dissolution of carbonate minerals, less time for water–rock interaction and short route of flow.

However, as the water infiltrates downwards, more and more chemical constituents are added and groundwater evolves and modifies to different water types depending upon flow path and host lithology.

Various scatter plots revealed the carbonate lithology as the main contributor of ions in the groundwater. However, Kongamnag showed the impact of silicate weathering also. Results of the physico-chemical analysis suggest that the karst springs and the Bringi stream have similar chemical composition. However, there are subtle differences in the major ion chemistry between the springs. Achabalnag and Kokernag located at lower altitudes have less ionic concentration as compared to the high-altitude spring (Kongamnag). The hydrographs and chemographs were plotted during different months in order to determine the type of discharged waters. In both streams and springs EC, TDS, Ca and HCO_3 were high during winter and low during summer. However, Kokernag and Achabalnag showed piston effect during July. The chemographs plotted during different months for streams and springs showed a positive correlation which indicated that springs are fed by the Bringi stream at different elevations.

1. Jeelani, G., Chemical quality of spring waters of Anantnag District, J&K, India. *J. Geol. Soc. India*, 2005, **66**, 453–462.
2. Jeelani, G., Hydrogeology of hard rock aquifer in Kashmir valley: complexities and uncertainties. In *Groundwater Dynamics in Hard Rock Aquifers – Including Sustainable Management and Optimal Monitoring Network Design* (eds Ahmad, S., Jayakumar, R. and Abdin, S.), Springer Verlag, The Netherlands, 2007, pp. 243–248.
3. Afsin, M., Hydrochemical evolution and water quality along the groundwater flow path in the Sandikli Plain, Afyon Turkey. *Environ. Geol.*, 1997, **31**, 221–230.
4. Ozdemir, M. and Nalbantcilar, M. T., The investigation of mass transfer in the karasu karstic aquifer, Konya, Turkey. *Hydrogeol. J.*, 2002, **10**, 656–661.
5. Freeze, R. A. and Cherry, J. A., *Groundwater*, Prentice Hall, N.J., 1979.
6. Panwar, S. and Chakrapani, G. J., Climate change and its influence on groundwater resources. *Curr. Sci.*, 2013, **105**, 37–46.
7. Jeelani, G., Bhat, N. A., Shivanna, K. and Bhat, M. Y., Geochemical characterization of surface water and spring water in SE Kashmir valley, western Himalayas: implication to water–rock interaction. *J. Earth Syst. Sci.*, 2011, **120**(5), 921–932.
8. Potter, P. E., Petrology and chemistry of big river sands. *J. Geol.*, 1978, **86**, 423–449.
9. Sarin, M. M., Krishnaswami, S., Dilli, K., Somayajulu, B. L. K. and Moore, W. S., Major ion chemistry of the Ganga–Brahmaputra river system: weathering processes and fluxes to the Bay of Bengal. *Geochim. Cosmochim. Acta*, 1989, **53**, 997–1009.
10. Jeelani, G., Aquifer response to regional climate variability in a part of Kashmir Himalaya in India. *Hydrogeol. J.*, 2008, **16**(8), 1625–1633.
11. Edmunds, W. M. and Smedley, P. L., Residence time indicators in groundwater: the East Midlands Triassic sandstone aquifer. *Appl. Geochem.*, 2000, **15**, 737–752.
12. Karim, A. and Veizer, J., Weathering processes in the Indus River Basin: implications from riverine carbon, sulfur, oxygen, and strontium isotopes. *Chem. Geol.*, 2000, **170**, 153–177.
13. Quade, J., English, N. and DeCelles, P. G., Silicate versus carbonate weathering in the Himalaya: a comparison of the Arunand Seti River watersheds. *Chem. Geol.*, 2003, **202**, 275–296.
14. Herczeg, A. I., Torgersen, T., Chivas, A. R. and Habermehl, M. A., Geochemistry of groundwater from the great Artesian Basin, Australia. *J. Hydrol.*, 1991, **126**, 225–245.
15. Bhat, N. A., Delineation of recharge areas of some karst springs of Anantnag using hydrogeochemistry and isotopes. M Phil dissertation, University of Kashmir, 2011; www.dspaces.uok.edu.in
16. Lawrence, W., *The Valley of Kashmir*, Kesar Publishers, 1967.
17. Jeelani, G., Bhat, N. A. and Shivanna, K., Use of $\delta^{18}O$ tracer to identify stream and spring origins of a mountainous catchment: a case study from Liddar watershed, western Himalaya, India. *J. Hydrol.*, 2010, **393**, 257–264.
18. Wadia, D. N., *Geology of India*, Tata McGraw Hill, New Delhi, 1975.
19. Middlemiss, C. S., A revision of Silurian–Triassic sequence of Kashmir. *Rec. Geol. Surv. India*, 1910, **40**(3), 6–260.
20. Coward, J. M. H., Waltham, A. C. and Bowser, R. J., Karst springs in the Vale of Kashmir. *J. Hydrol.*, 1972, **16**, 213–223.
21. Bhatt, D. K., On the Quaternary geology of Kashmir Valley with special reference to stratigraphy and sedimentation. *Geol. Surv. India, Misc. Publ.*, 1975, **24**(1), 188–203.
22. Jeelani, G., Effect of subsurface lithology on hydrochemistry of springs of a part of Kashmir Himalaya. *Himalayan Geol.*, 2004, **25**(2), 145–151.
23. APHA, *Standard Method for Examination of Water and Wastewater*, APHA, AWWA, WPCF, Washington, 2005, 21st edn.
24. Goldscheider, N. and Drew, D., *Methods in Karst Hydrogeology*, Taylor and Francis, London. 2007.
25. Clark, I. D. and Fritz, P., *Environmental Isotopes in Hydrogeology*, Lewis Publishers, Boca Raton, USA, 1997.
26. Singh, S. K., Sarin, M. M. and France-Lanord, C., Chemical erosion in the eastern Himalaya: major ion composition of the Brahmaputra and $\delta^{13}C$ of dissolved inorganic carbon. *Geochim. Cosmochim. Acta*, 2005, **69**, 3573–3588.
27. Hiscock, K. M., The influence of pre-Devensian deposits on the hydrogeochemistry of chalk aquifer system of North Norfolk, UK. *J. Hydrol.*, 1993, **144**, 355–369.
28. Kimblin, R. T., The chemistry and origin of groundwater in Triassic sandstone and Quaternary deposits, northwest England and some UK comparison. *J. Hydrol.*, 1995, **172**, 293–311.
29. Elliot, T., Andrews, J. N. and Edmunds, W. M., Hydrochemical trends, paleorecharge and groundwater ages in the fissured Chalk aquifer of London and Berkshire Basins. *Appl. Geochem.*, 1999, **14**, 333–363.
30. Gibbs, R. J., Mechanisms controlling world water chemistry. *Science*, 1970, **170**, 1088–1090.
31. Piper, A. M., A graphical procedure in the geochemical interpretation of water analysis. *Trans. Am. Geophys. Union*, 1994, **25**, 914–928.
32. Langelier, W. E. and Ludwig, H. F., Graphical method for indicating the mineral character of natural water. *J. Am. Water Works Assoc.*, 1942, **34**, 335–352.
33. Frondini, F., Geochemistry of regional aquifer systems hosted by carbonate–evaporite formations in Umbria and southern Tuscany (central Italy). *Appl. Geochem.*, 2008, **23**(8), 2091–2104.

Received 22 December 2013; revised accepted 3 March 2014